XMM-Newton CCF Release Note

XMM-CCF-REL-305

EPIC-MOS contamination parameters

S. Sembay & R. Saxton

September 4, 2013

1 CCF components

Name of CCF	VALDATE	List of Blocks changed	Change in CAL HB
EMOS1_CONTAMINATION_0001.CCF	2000-01-01	CONTAM_DEPTH	YES
EMOS2_CONTAMINATION_0001.CCF	2000-01-01	CONTAM_DEPTH	YES

2 Change

It has become apparent that the response of the MOS cameras (primarily MOS2) has deteriorated at low-energies (< 1 keV) over the course of the mission. It is suspected that this is due to contaminants which have adhered to the surface of the cameras, absorbing a fraction of the incoming photons. These new CCF elements tabulate the depths of contaminating elements as a function of time (see Tab. 1). Depths have been tabulated from the beginning of the mission (2000-01-01) and extrapolated until 2028-07-06. Carbon, Oxygen and Fluorine are common components of measured contaminants on some other X-ray instruments (e.g. ACIS on Chandra). In this release the entries in the CCF for Oxygen and Fluorine are placeholders and have zero depth. The MOS contaminant is currently modelled as pure Carbon, similar to that observed on the RGS. There is no evidence for a contaminant on the pn camera.

2.1 Determination of the contaminant

Figure 1 shows the observed count rate ratio in the 0.1-0.75 keV to 0.98-3.0 keV bands from observations of the SNR 1E0102.2-7219, which is known to have a highly stable spectrum. Different positions of the source on the detector are indicated by the color coding (see figure caption). Part of the scatter in the ratio is due to position-dependent effects such as vignetting and charge redistribution, while the strong trend with revolution number, seen in MOS2, may only be plausibly

Table 1: CCF column description

Column name	Desciption
TIME	observation date (MJD)
C_DEPTH	depth of carbon in microns
O_DEPTH	depth of oxygen in microns
F_DEPTH	depth of flourine in microns

explained by the existence of a thin but growing contaminant. The evidence for a temporal trend in the MOS1 data is marginal. Similar trends are observed in the SNR N132D which also has a long baseline of observations.

The continuous line on each plot shows the ratio which is predicted if the effective area (which already accounts for position-dependent effects) is modified by an evolving Carbon absorber. The depth of this material (in microns) is shown, as a function of time, in Figure 2. In Fig. 2 the points show the thickness of Carbon required to produce a 0.1-0.75 keV to 0.98-3.0 keV count rate ratio equal to that predicted by the standard IACHEC model of this source (Plucinsky et al. 2012). These points have then been fitted with an exponential model to give a smooth deposition of contaminant (although in the current epochs it appears to the eye to be fairly linear).

Note that directly observing a well-defined carbon edge in continuum sources is not possible due to the complicated shape of the RMF at low energies.

All measurements were taken within 2 arcminutes of the camera optical-axis. It is assumed that the contaminant has been deposited uniformly over the field of view and hence no spatial dependency has been introduced into the calibration.

3 Scientific impact of this update

The effective area of the MOS cameras, calculated by the task *arfgen*, will be reduced at energies < 1 keV. In practise, the major effect will be around the Carbon edge, between $\sim 300 - 500$ eV, which will experience a reduction in the effective area, and a consequent rise in measured flux, in this energy range, of $\sim 10\%$ for observations taken in 2013 with MOS-2. The effect will be less for earlier observations and for those made with MOS-1.

4 Estimated scientific quality

This change should lead to a more consistent cross-calibration between the three EPIC cameras than is presently available, especially at later epochs.

To test this we have fit the EPIC-pn and MOS-2 spectra of 3C 273 from revolution 2308 with

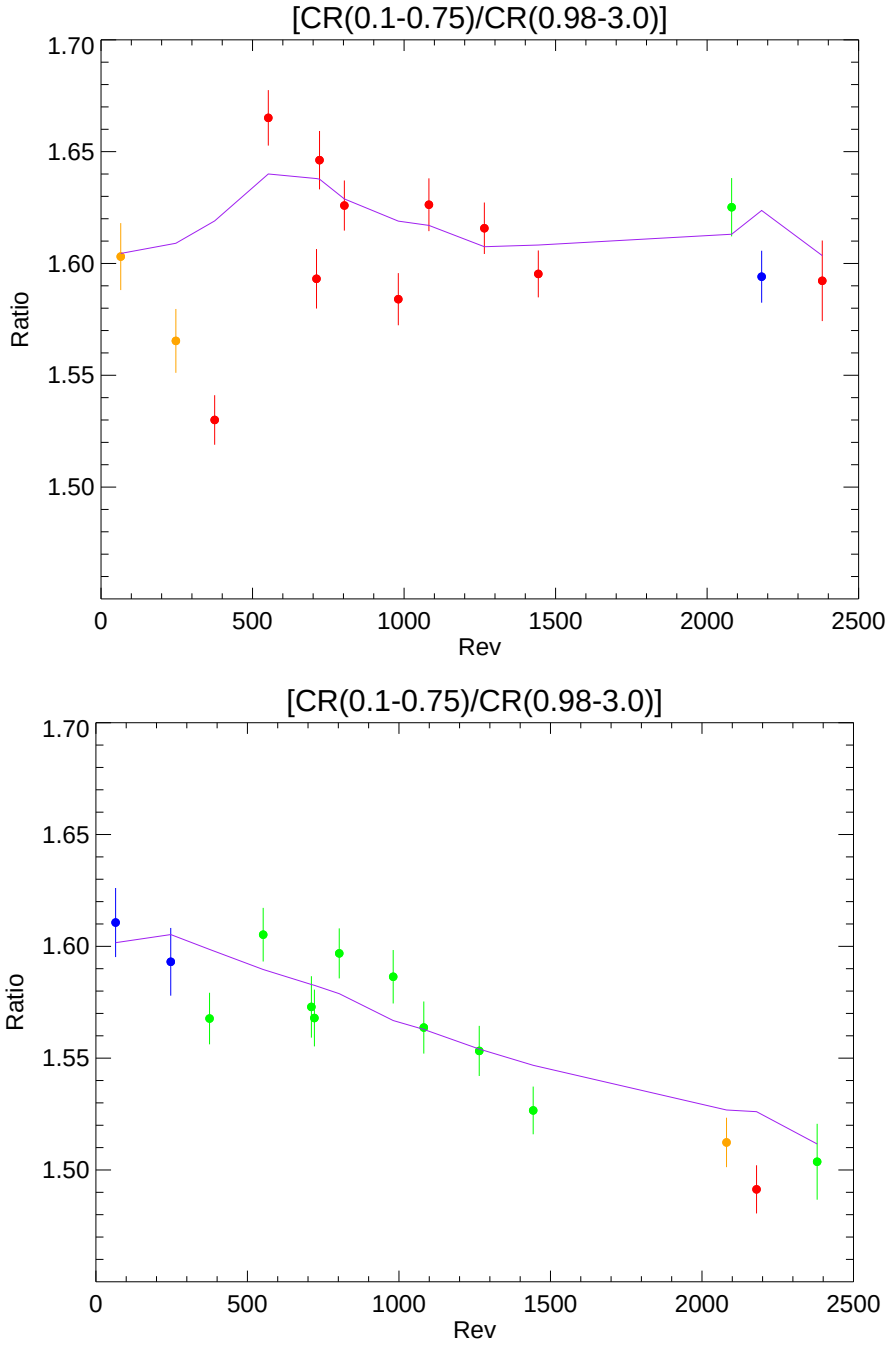

Figure 1: The 0.1–0.75 keV / 0.98–3.0 keV count rate ratio from the SNR 1E0102.2-7219 as a function of the revolution number; upper (MOS-1), lower (MOS-2). Points are colour-coded to reflect the position of the source on the detector relative to the boresight: blue(above boresight), orange (to the right), green (below), red (to the left). The solid blue line represents the expected ratio after correcting for position-dependent effective area differences and a film of Carbon contaminant, whose depth increases over the course of the mission.

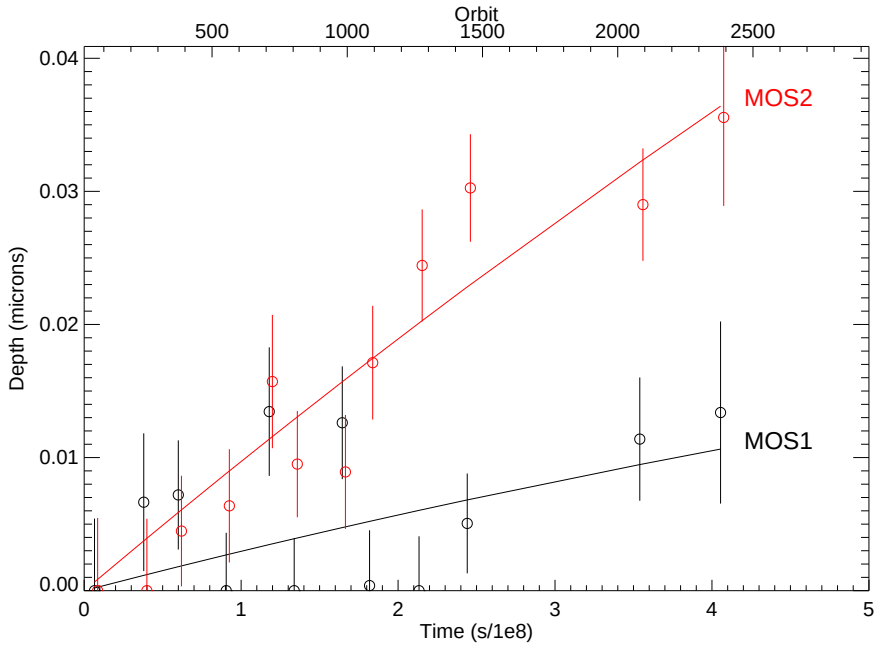

Figure 2: The depth of Carbon contaminant, in microns, inferred to lie on the MOS cameras as a function of observation time (offset from 2000-01-01T12:00:00). Solid curves represent a best-fit exponential model.

a model of a double power-law, absorbed by the galactic column and multiplied by an instrument-dependent constant (Fig. 3). The new effective area, including a correction for absorption by a layer of Carbon, gives a better agreement between the EPIC-pn and MOS-2 data.

5 Test procedure and results

These CCFs will be used by the task *arfgen* to calculate the total effective area of the MOS cameras including the effects of contamination. We have ran the task for the two cameras on data from 2000-01-01 and from 2013-01-01. The difference in the effective areas can be seen in figure 4.

6 Future changes

The depths have been extrapolated into the future using an exponential model. This should be reviewed periodically to ensure that the deposition of the contaminant(s) continues at the expected rate.

Should sufficient high-quality data become available for off-axis sources it may be possible to test the spatial dependency of the contamination over the field of view.

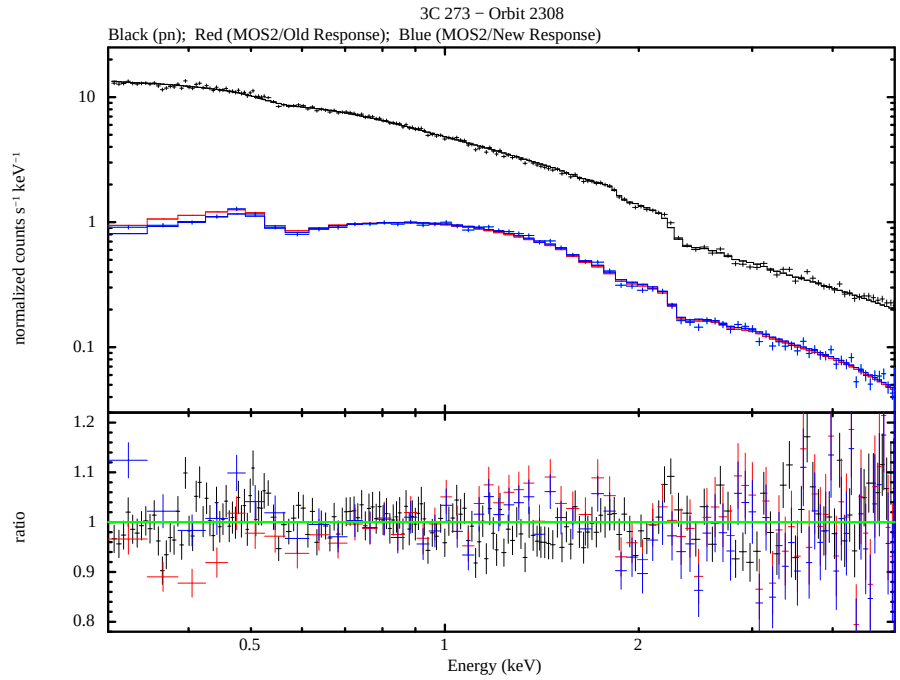

Figure 3: A fit to an observation of the QSO 3C273 from revolution 2308 with an absorbed double power-law model. The model was first fit to the EPIC-pn points (black) and then applied to the MOS-2 data, using the original effective area file (red) and an effective area corrected for contamination (blue).

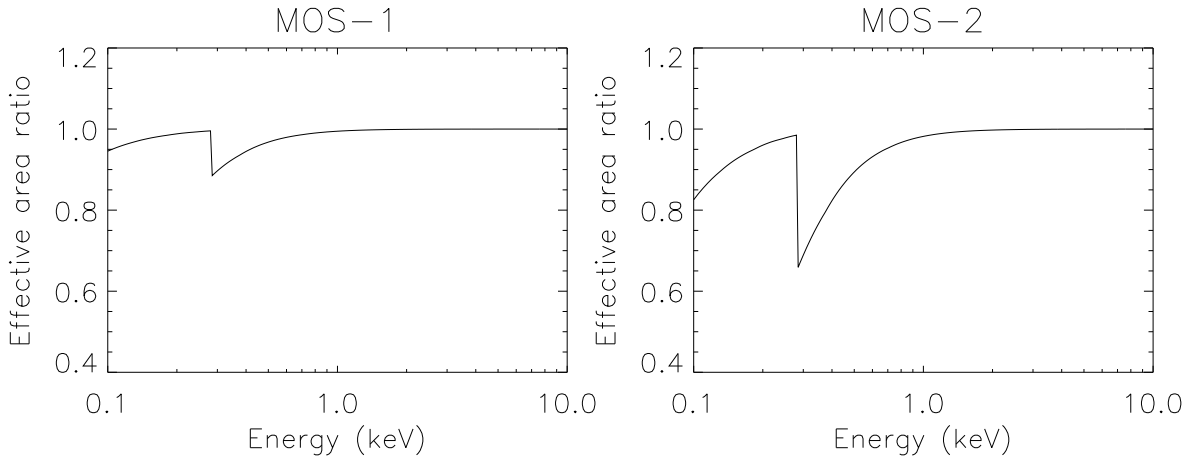

Figure 4: The ratio of effective areas between two observations taken in 2013-01-01 and 2000-01-01 for MOS-1 (left) and MOS-2 (right). The ratios are due to the contamination layers which have formed on the MOS cameras since launch. This is much deeper in the MOS-2 camera.

7 References

P.P.Plucinsky et al. *"Cross-calibration of the x-ray instruments onboard the Chandra, Suzaku, Swift, and XMM-Newton Observatories using the SNR 1E 0102.2-7219"*, 2012, SPIE, 8443, 12